Erciyes Med J 2021; 43(5): 487–93 • DOI: 10.14744/etd.2021.25593
ORIGINAL ARTICLE – OPEN ACCESS

Characterization of Cancer Immune Landscape in Primary Central Nervous System Lymphoma

Fei Fei[1], Kai Wang[1], Deniz Peker[2]

ABSTRACT

Objective: Primary central nervous system lymphoma (PCNSL) is a rare and aggressive extranodal variant of non-Hodgkin lymphomas with disease confined to the brain, spinal cord, leptomeninges, or orbit, without evidence of systemic involvement. PCNSL has a poor prognosis, with a median overall survival of 30–50 months. We used NanoString Technologies to characterize the cancer immune profiles in PCNSL and associated the findings with clinical outcome.

Materials and Methods: A total of 33 patients between 2005 and 2017 were included in our study, and clinical information was collected. A PanCancer IO 360 panel (NanoString Technologies) was used to assess the expression level of 770 genes related to tumor immunity in 12 samples. We also investigated the programmed death ligand 1 (PD-L1) expression and T-cell infiltrate in 25 PCNSL samples using immunohistochemistry.

Results: NanoString analysis showed that gene expressions differed between human immunodeficiency virus (HIV)-positive and HIV-negative PCNSL. We identified four genes with deregulated expressions (adjusted $p<0.05$) with a cluster enrichment in cytotoxicity, DNA damage repair, interferon signaling, and lymphoid compartment-related genes. Furthermore, we found that PD-L1 was expressed in 9 of 25 (36%) cases and 11 had increased CD3+ T-cell infiltrates. However, increased PD-L1 expression and CD3+ T-cell infiltrates were not correlated with the clinical outcome.

Conclusion: Our data reveals a distinct PCNSL tumor microenvironment and immune landscape. However, our study needs to be validated in a larger population.

Keywords: Primary central nervous system lymphoma, PD-L1, tumor microenvironment

Cite this article as:
Fei F, Wang K, Peker D. Characterization of Cancer Immune Landscape in Primary Central Nervous System Lymphoma. Erciyes Med J 2021; 43(5): 487-93.

[1]Department of Pathology, University of Alabama at Birmingham, Birmingham, AL, USA
[2]Department of Pathology, Emory University Faculty of Medicine, Atlanta, GA, USA

Submitted
15.11.2020

Accepted
31.01.2021

Available Online
05.08.2021

Correspondence
Deniz Peker,
Emory University Faculty of Medicine, Department of Pathology, 1364 Clifton Road, Atlanta, GA 30322
Phone: +1 404 712 3855
e-mail:
deniz.peker@emory.edu

INTRODUCTION

Primary central nervous system lymphoma (PCNSL) is a rare form of non-Hodgkin B-cell lymphoma(s) limited to the brain, spinal cord, leptomeninges, and/or orbital cavity, without evidence of systemic involvement (1, 2). PCNSL is an aggressive disease with a poor prognosis and a median overall survival (OS) of 30–50 months. In addition, the risk of recurrence is near 50% within the first 2 years of diagnosis, and one-third of patients with PCNSL are refractory to initial treatment (2–4). High-dose methotrexate-based immunochemotherapy induction therapy followed by consolidation including whole-brain radiotherapy, nonmyeloablative chemotherapy, and high-dose chemotherapy with autologous stem cell transplantation is a widely adopted choice of treatment. However, no standard therapeutic approach has been established for relapsed/refractory disease.

In recent years, novel treatment options based on microenvironment and immune response have been investigated for patients with relapsed/refractory PCNSL, particularly anti-programmed death 1 (PD-1) therapy (5). PD-1, also known as cluster of differentiation 179, is an immune receptor belonging to the immunoglobulin superfamily (6, 7). PD-1 is expressed in several immune cells, particularly activated T lymphocytes, B lymphocytes, and myeloid cells, to modulate their activation of inhibition (7). Programmed death ligand 1 (PD-L1) is one of the most significant PD-1 ligands that is expressed in tumor cells and other immune cells. It was demonstrated that the inhibitory effect of PD-L1 is accomplished through a mechanism that enables tumor cells to escape immunity by inactivating cytotoxic T cells and/or inhibiting tumor cell apoptosis (8). Previous studies revealed frequent 9p24.1/PD-L1 (CD274)/PD-L2 (PDCD1LG2) copy number alterations resulting in increased expression levels of PD-1 ligands PD-L1 or PD-L2 in PCNSL (2, 9). Furthermore, chromosomal rearrangements involving PD-L1 or PD-L2 and selective overexpression of the respective ligand were identified in PCNSL in these studies. Nayak et al. also reported clinical response with PD-1 blockade using nivolumab in four patients with relapsed/refractory PCNSL (2, 9).

A strong correlation between tumor microenvironment and limited immune surveillance on lymphoma pathogenesis and survival has been recognized (9,10); however, our knowledge of tumor microenvironment and its roles in clinical behavior in PCNSL is limited. In this study, we aimed to characterize the cancer immune profiles in cases with PCNSL and correlate the findings with clinical outcome(s).

Table 1. Clinicopathologic characteristics of PCNSL cases analyzed using NanoString (n=12)

No	Age (year)	Sex	Tumor location	Other sites involved	Treatment	HIV status	CD20 (IHC)	CD10 (IHC)	BCL6 (IHC)	MUM1 (IHC)	LDH levels (Units/L)
1	84	M	Right thalamic	None	RTx	-	+	N/A	+	+	214.00
2	68	M	Spine	Thoracic	CTx	-	+	+	N/A	N/A	179.00
3	31	F	Left frontal	None	CTx	+	+	+	N/A	N/A	140.00
4	62	F	Left frontal	None	STx + CTx	-	+	+	+	-	N/A
5	61	F	Right temporal	None	RTx + CTx + STx	-	+	-	-	+	172.00
6	54	F	Right temporal	None	CTx	-	+	-	+	+	294.00
7	73	F	Left frontal	None	RTx + CTx + STx	-	+	-	N/A	N/A	203.00
8	66	M	Right thalamic	None	CTx	-	+	N/A	+	N/A	100.00
9	84	M	Cervical spine	None	RTx + CTx	-	+	+	+	N/A	140.00
10	38	F	Right temporal	None	CTx	+	+	N/A	-	+	226.00
11	54	M	Right frontal	None	STx + CTx	-	+	N/A	N/A	N/A	147.00
12	78	F	Left occipital	None	CTx	-	+	N/A	N/A	N/A	313.00

HIV: Human immunodeficiency virus; IHC: Immunohistochemical; LDH: Lactate dehydrogenase; M: Male; F: Female; N/A: Not applicable

MATERIALS and METHODS

Case Selection

From 2004 to 2017, 33 patients diagnosed and treated with PCNSL including immunodeficiency-associated PCNSL were identified at the University of Alabama at Birmingham. Formalin-fixed paraffin-embedded (FFPE) blocks were retrieved from the Department of Pathology archives. Demographic, clinical, and pathological data were collected by a retrospective electronic medical record review. This study was approved by the Institutional Review Board of the University of Alabama at Birmingham.

NanoString Assay for Gene Expression

Adequate tumor sample (three 2-mm punch biopsies for each case) was successfully obtained from 12 FFPE blocks. RNA was isolated from dissected tumor tissue using the RNeasy FFPE Kit (Qiagen, Valencia, CA) according to the manufacturer's instructions. RNA quantity and quality were assessed via the 260/280 ratio by NanoDrop. A total of 100 ng of RNA was input directly into the nCounter® platform (NanoString Technologies, Seattle, WA) for the hybridization with PanCancer IO 360 panel, which included 770 immune-related genes (NanoString Technologies, Seattle, WA) as previously described (11). Data were collected and processed as by the nCounter® Digital Analyzer (NanoString Technologies, Seattle, WA) as previously described (12).

After completion of normalization process, counts were log2 transformed, and a build ratio analysis was performed by comparing the expression profiles of human immunodeficiency virus (HIV)-positive and HIV-negative samples using nSolver 3.0 software (NanoString Technologies, Seattle, WA). Bioinformatic analyses on gene expression profiling (GEP) was conducted by the nCounter® Advanced Analysis (NanoString Technologies, Seattle, WA).

Immunohistochemistry

Immunohistochemical (IHC) staining was performed on 25 cases according to standard methods at the UAB Core Laboratory. Briefly, 4-µm sections were obtained from FFPE tissue blocks, and the staining was performed using a semiautomated immunostainer (Leica Biosystems, Buffalo Grove, IL) with antibodies against CD20 (Clone L26, Leica) and CD3 (Clone LN10, Leica) as previously described (13). PD-L1 (1:100 dilution, clone E1L3N; Cell Signaling Technology, Danvers, MA) IHC stain was also performed according to the manufacturer's instruction (14).

The evaluation of PD-L1 and CD3 expression was performed manually by two investigators (FF and KW). At least 10 high-power fields (HPFs) in each case were evaluated in areas dominated by tumor cells. PD-L1-positive cases were defined as ≥5% of the tumor cells showing distinct membranous and/or cytoplasmic staining in moderate (5%–30%) or strong (≥30%) intensity as previously described in the literature (15). A cutoff of 5% was chosen based on the previous studies (16–18). The quantification of CD3+ T cells was performed manually in average 10 HPFs. T-cell infiltration pattern was divided into two groups: low CD3+ T-cell infiltrates (<25%) and high CD3+ T-cell infiltrates (≥25%).

Statistical Analyses

The Kaplan–Meier survival curves and log-rank tests were performed to compare survival times between groups using GraphPad Prism software (version 5.0). GEP analysis was evaluated by adjusted p value (Benjamini–Hochberg procedure). A p value of <0.05 was considered statistically significant.

RESULTS

Characterization of Immune Landscape in PCNSL Using NanoString

Twelve patients were included in this part of the study. The patients' clinicopathological data are summarized in Table 1. Among the 12 patients, 10 were diagnosed with HIV-negative PCNSL, while 2 were diagnosed with HIV-positive PCNSL. EBV status was available in three cases; one case was positive via EBV-encoded small RNA in situ hybridization (EBER), while the other two cases were negative. The male-to-female ratio was 5:7, and the median age was 64 (range, 31–84) years.

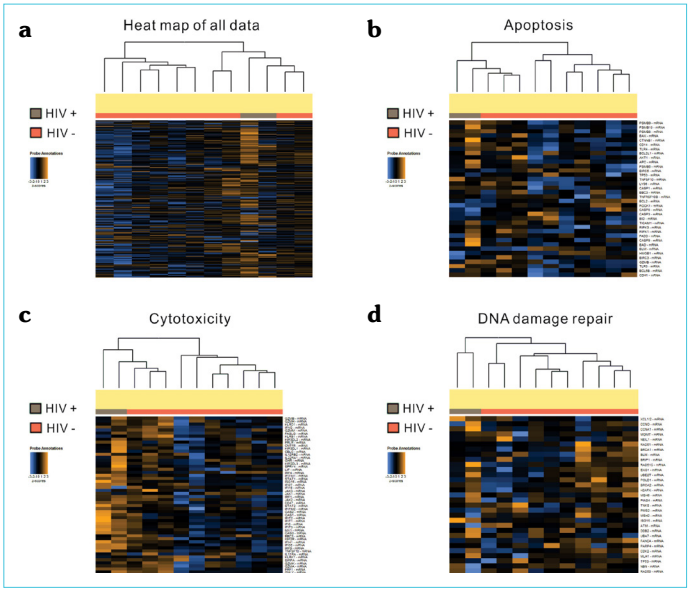

Figure 1. The NanoString PanCancer IO 360 panel highlights different gene expression profiles between human immunodeficiency virus (HIV)-negative and HIV-positive groups. (a) Heatmap of all data between HIV-negative and HIV-positive groups. (b). Heatmap of apoptosis-related genes. (c) Heatmap of cytotoxicity-related genes. (d) Heatmap of DNA damage repair-related genes

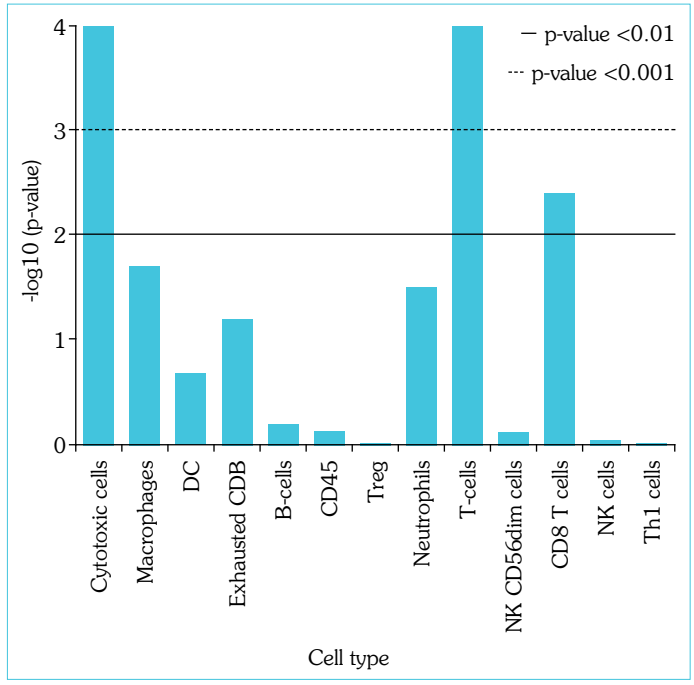

Figure 2. Cell type analysis between human immunodeficiency virus (HIV)-negative and HIV-positive primary central nervous system lymphomas (p values are–log10 transformed)

Twelve patients were divided into two groups according to the HIV status and GEP in a panel of 770 immune-related genes that were analyzed. As shown in Figure 1a, hierarchical clustering indicated difference in gene expressions between HIV-positive and HIV-negative groups, particularly for the genes associated with apoptosis, cytotoxicity, and DNA damage repair (Fig. 1b–d). Differential analysis between HIV-positive and HIV-negative subgroups identified 127 significantly deregulated genes ($p<0.05$), including 83 upregulated and 44 downregulated genes. The significance of these 127 genes was reanalyzed by adjusted p values (Benjamini–Hochberg procedure), and only 4 genes (HERC6, ISG15, OAS2, and IFIT1) were identified to be significantly deregulated (adjusted p value <0.05). The top 20 genes with expression abnormalities are listed in Table 2. We believe that the difference between p value and the adjusted P value was due to the limited sample size. Further analysis showed enrichment in cytotoxicity, DNA damage repair, interferon signaling, and lymphoid compartment-related genes (Table 2). Cell type profile analysis highlighted that the cytotoxic cells, T cells, and CD8+ T cells were significantly associated with both HIV-positive and HIV-negative groups (Fig. 2).

PD-L1 Expression and CD3+ T-Cell Infiltrates

Twenty-five cases were included in the IHC study. The patients' characteristics are summarized in Table 3. There were 16 male (64%) and 9 female (36%) patients. The median age was 62 (range, 25–84) years. The HIV test results were positive in 8 patients (32%), negative in 16 patients (64%), and unknown in 1 patient (4%). The mean follow-up period was 36 (range, 1.0–143) months.

In all cases, tumor cells stained positive with CD20 confirming the B-cell origin. The PD-L1 expression levels were determined based on the membranous and/or cytoplasmic staining (Fig. 3). Of the 25 cases, 9 (36%) were positive for PD-L1 expression in tumor cells with 5 cases (20%) showing moderate and 4 cases (16%) showing strong PD-L1 staining (Table 3). Interestingly, a strong PD-L1 expression was observed mostly in perivascular regions (Fig. 3). We also compared PD-L1 expression between HIV-positive and HIV-negative cases; however, no significant difference was identified, which was likely due to the small number of cases (data not shown). Next, we evaluated the CD3+ T-cell infiltration in tumor microenvironment. As shown in Table 3, 11 cases (44%) had a high number of CD3+ T cells (≥25%), while 14 cases (56%) had a low number of CD3+ T cells (<25%). Similar to PD-L1 expression, the CD3+ T-cell infiltrate level was not associated with the HIV status (data not shown).

Correlation Between HIV Status, PD-L1 Expression, and CD3+ T-Cell Infiltrate and Clinical Outcome

The median OS of all patients was 36.1 (range, 1–143) months. We evaluated the prognostic significance of HIV status, PD-L1 expression, and CD3+ T-cell infiltrate in PCNSL. As indicated in Figure 4, HIV status (p=0.4560), PD-L1 expression (p=0.9352), and CD3+ T-cell infiltrate (p=0.7540) were not correlated with OS.

DISCUSSION

Clinical management of PCNSL is still challenging especially for patients with relapsed/refractory disease, indicating the necessity for novel biomarkers and more effective treatment options. A greater level of understanding of the immune profile and microenvironment in PCNSL may facilitate the development and application of targeted therapies in these patients.

Table 2. The genes with significant expression alterations in HIV-negative HIV-positive PCNSL

Gene (mRNA)	Log2 fold change	Std error (log2)	Lower confidence limit (log2)	Upper confidence limit (log2)	p value	Ajusted p value	Gene sets	Probe ID
HERC6	2.91	0.472	1.98	3.83	0.000107	0.0365	NM_001165136.1:883	
ISG15	4.48	0.732	3.05	5.92	0.000112	0.0365	Cytotoxicity, DNA Damage Repair, Interferon Signaling, Lymphoid Compartment	NM_005101.3:305
OAS2	2.59	0.451	1.71	3.47	0.000187	0.0405	Cytotoxicity, Interferon Signaling	NM_016817.2:380
IFIT1	5.11	0.929	3.29	6.93	0.00026	0.0411	Cytotoxicity, Interferon Signaling, Lymphoid Compartment	NM_001270930.1:1675
IL16	-1.74	0.325	-2.38	-1.11	0.000316	0.0506	Cytokine and Chemokine Signaling	NM_004513.4:1262
EIF2AK2	2.08	0.414	1.27	2.89	0.000523	0.0506	Interferon Signaling	NM_001135652.2:516
RSAD2	4.59	0.936	2.75	6.42	0.000623	0.0506	Interferon Signaling	NM_080657.4:1057
CD1C	-7.19	1.47	-10.1	-4.3	0.000639	0.0506	Antigen Presentation, Lymphoid Compartment	NM_001765.2:564
FCRL2	-4.48	0.944	-6.33	-2.63	0.000785	0.0506		NM_001159488.1:132
CD79B	-4	0.845	-5.66	-2.34	0.000801	0.0506	Lymphoid Compartment	NM_001039933.1:884
IRF9	1.43	0.311	0.823	2.04	0.00097	0.0506	Cytotoxicity, Interferon Signaling, JAK-STAT Signaling, Lymphoid Compartment	NM_006084.4:723
OAS3	3.54	0.772	2.03	5.05	0.000995	0.0506	Cytotoxicity, Interferon Signaling	NM_006187.3:2354
IRF7	2.12	0.467	1.2	3.04	0.00108	0.0506	Interferon Signaling	NM_004029.2:1705
IFI35	2.33	0.515	1.32	3.34	0.0011	0.0506	Cytotoxicity, Interferon Signaling	NM_005533.4:729
SPIB	-3.69	0.824	-5.31	-2.08	0.00117	0.0506		NM_003121.3:1029
FSTL3	3.46	0.781	1.93	4.99	0.00126	0.0512	Angiogenesis	NM_005860.2:255
LILRA5	3.77	0.895	2.02	5.53	0.00177	0.0563	Myeloid Compartment	NM_181879.2:545
IFIH1	2.3	0.546	1.23	3.37	0.00179	0.0563	Cytotoxicity, Interferon Signaling	NM_022168.3:3250
IFI6	3.92	0.932	2.1	5.75	0.0018	0.0563	Cytotoxicity, Interferon Signaling	NM_002038.3:410
CLECL1	-2.8	0.667	-4.1	-1.49	0.00184	0.0563	Immune Cell Adhesion and Migration	NM_172004.3:357

PCNSL: Primary central nervous system lymphoma; HIV: Human immunodeficiency virus

Table 3. Clinicopathologic characteristics of PCNSL cases studied using immunohistochemistry (n=25)

	Total (n)	Median	Range
Patients	25		
Gender			
Male	16 (64%)		
Female	9 (36%)		
Age		62	25–84
HIV status			
Positive	8 (32%)		
Negative	16 (64%)		
N/A	1 (4%)		
Infiltration CD3 + T cell			
High (>25%)	11 (44%)		
Low (≤25%)	14 (56%)		
PO-L 1 expression			
Negative: <5%	16 (64%)		
Moderate: 5–30%	5 (20%)		
Strong: >30%	4 (16%)		

4 patients from previous Nanostring studie were included in this study. PCNSL: Primary central nervous system lymphoma; HIV: Human immunodeficiency virus

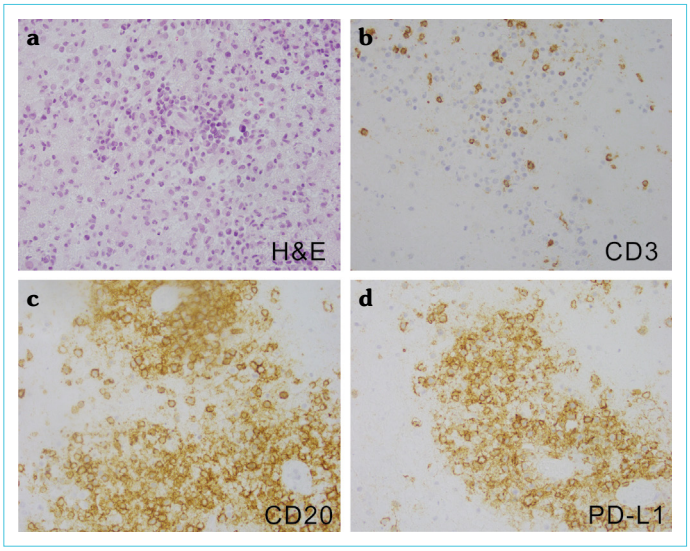

Figure 3. Histopathologic and immunophenotypic characteristics of primary central nervous system lymphoma cells using hematoxylin and eosin (a), CD3 (b), CD20 (c), and programmed death ligand 1 (d)

In this study, we investigated the unique characteristics of tumor microenvironment PCNSL using a comprehensive gene panel applied by NanoString Technologies. Interestingly, our results showed remarkable deregulations in genes clustered in cytotoxicity, DNA damage repair, interferon signaling, cytokine and chemokine signaling, and lymphoid compartments. Additionally, our data suggests that the PCNSL immune profile differs between immunocompetent and immunocompromised patients, which could be linked to different pathogenic mechanisms in this lymphoma.

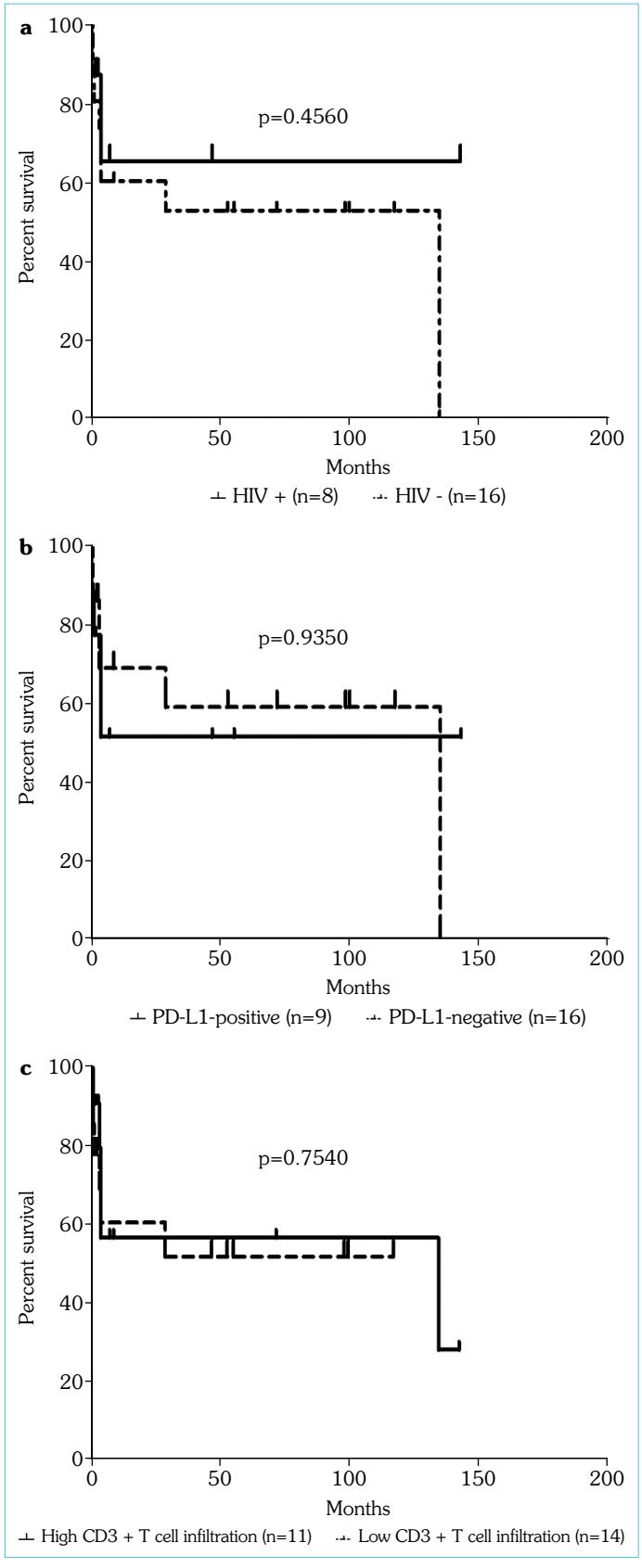

Figure 4. Kaplan–Meier survival analysis results. A. Comparing patients based on the human immunodeficiency virus status (a), programmed death ligand 1 expression (b), and low versus high CD3+ T-cell infiltrates (c)

PD-1 and PD-L1 expression has been recently reported in diffuse large B-cell lymphoma (DLBCL), classical Hodgkin lymphoma, follicular lymphoma, and chronic lymphoblastic leukemia (19–26); however, only limited data is available regarding PD-L1 expression in PCNSL (16, 27, 28). Cho et al. (28) analyzed 76 PCNSL cases and found an increased expression of PD-L1 in 71.1% (54/76) of patients. The results of this study also indicated that the PD-L1 expression levels in tumor cells were not correlated with survival. Furuse et al. (27) illustrated that among 70 patients with PCNSL, 19 (27.1%) showed strong or moderate PD-L1 expression in tumor cells with no statistically significant correlation between PD-L1 positivity and clinical outcome. However, they noticed that PD-L1 expression on peritumoral macrophages was strongly predictive of a favorable outcome. The study performed by Berghoff et al. (16) showed strong PD-L1 expression in lymphoma cells in 2 of 20 (10%) PCNSL cases. Interestingly, the authors reported that a strong PD-L1 expression was most marked in the perivascular region. In our study, we found that PD-L1 was expressed in 9 of 25 (36%) PCNSL cases, with a strong (≥30%) PD-L1 expression in 4 (16%) cases. Similar to results of Berghoff's study (16), a strong PD-L1 staining was observed mostly in the perivascular regions in our cases. In accordance with previous studies (27, 28), the PD-L1 expression was not correlated with clinical outcome. However, we noticed that there is no standardized method to evaluate PD-L1 expression and each study may use different commercial PD-L1 antibodies, which may cause the wide range of PD-L1 expression levels in PCNSL.

Additionally, we investigated the level of CD3+ T-cell infiltration in PCNSL since it was reported that T lymphocytes, mostly comprising CD4+ and CD8+ T cells, play a key role in cell-mediated immunity (10). Xu-Monette et al. (29) studied immune profile in 405 DLBCL samples, and their results showed that very low CD3+ T-cell infiltration (0%–2.6%) was associated with decreased progression-free survival and OS. Ciavarella et al. (30) demonstrated that the presence of a higher proportion of myofibroblasts, dendritic cells, and CD4+ T cells is not correlated with better outcome in patients with DLBCL (n=175). Pollari et al. (11) found that lower amounts of tumor-infiltrating CD4+ and CD8+ T cells were associated with a less favorable outcome in primary testicular lymphoma. Our results did not demonstrate a significant impact of CD3+ T-cell infiltrates to OS in patients with PCNSL. We believe that this may be due to the small sample size of the current study and the heterogeneous nature of the treatment regimens that were administered to our patient cohort.

In conclusion, we report a difference in tumor immune landscape between HIV-negative and HIV-positive PCNSL. PD-L1 expression was demonstrated in PCNSL; however, neither PD-L1 expression nor CD3+ T-cell infiltrate was associated with OS. Our results point that PCNSL harbors a distinct tumor microenvironment, which further differs between immunocompetent and immunocompromised groups. Future investigation of the role of immune landscape and microenvironment in PCNSL is justified, and large-scale studies are warranted.

Ethics Committee Approval: This study was approved by the Institutional Review Board of the University of Alabama at Birmingham (date: 19.03.2017, number: 300001574).

Peer-review: Externally peer-reviewed.

Author Contributions: Concept – DP, FF; Design – FF, DP; Supervision – DP; Resource – DP; Materials – FF; Data Collection and/or Processing – DP, FF, KW; Analysis and/or Interpretation – DP, FF, KW; Literature Search – DP, FF; Writing – FF, DP; Critical Reviews – DP.

Conflict of Interest: The authors have no conflict of interest to declare.

Financial Disclosure: The study was funded by the UAB Department of Pathology and Laboratory Medicine Adams Funds.

REFERENCES

1. Schaff LR, Grommes C. Updates on primary central nervous system lymphoma. Curr Oncol Rep 2018; 20(2): 11. [CrossRef]
2. Nayak L, Iwamoto FM, LaCasce A, Mukundan S, Roemer MGM, Chapuy B, et al. PD-1 blockade with nivolumab in relapsed/refractory primary central nervous system and testicular lymphoma. Blood 2017; 129(23): 3071–3. [CrossRef]
3. Langner-Lemercier S, Houillier C, Soussain C, Ghesquières H, Chinot O, Taillandier L, et al. Primary CNS lymphoma at first relapse/progression: characteristics, management, and outcome of 256 patients from the French LOC network. Neuro Oncol 2016; 18(9): 1297–303.
4. Korfel A, Schlegel U. Diagnosis and treatment of primary CNS lymphoma. Nat Rev Neurol 2013; 9(6): 317–27. [CrossRef]
5. Illerhaus G, Schorb E, Kasenda B. Novel agents for primary central nervous system lymphoma: evidence and perspectives. Blood 2018; 132(7): 681–8. [CrossRef]
6. Dong Y, Sun Q, Zhang X. PD-1 and its ligands are important immune checkpoints in cancer. Oncotarget 2017; 8(2): 2171–86. [CrossRef]
7. Goodman A, Patel SP, Kurzrock R. PD-1-PD-L1 immune-checkpoint blockade in B-cell lymphomas. Nat Rev Clin Oncol 2017; 14(4): 203–20.
8. Liu J, Quan L, Zhang C, Liu A, Tong D, Wang J. Over-activated PD-1/PD-L1 axis facilitates the chemoresistance of diffuse large B-cell lymphoma cells to the CHOP regimen. Oncol Lett 2018; 15(3): 3321–8.
9. Chapuy B, Roemer MG, Stewart C, Tan Y, Abo RP, Zhang L, et al. Targetable genetic features of primary testicular and primary central nervous system lymphomas. Blood 2016; 127(7): 869–81. [CrossRef]
10. Scott DW, Gascoyne RD. The tumour microenvironment in B cell lymphomas. Nat Rev Cancer 2014; 14(8): 517–34. [CrossRef]
11. Leivonen SK, Pollari M, Brück O, Pellinen T, Autio M, Karjalainen-Lindsberg ML, et al. T-cell inflamed tumor microenvironment predicts favorable prognosis in primary testicular lymphoma. Haematologica 2019; 104(2): 338–46. [CrossRef]
12. Ghatalia P, Gordetsky J, Kuo F, Dulaimi E, Cai KQ, Devarajan K, et al. Prognostic impact of immune gene expression signature and tumor infiltrating immune cells in localized clear cell renal cell carcinoma. J Immunother Cancer 2019; 7(1): 139. Erratum in: J Immunother Cancer 2019; 7(1): 273. [CrossRef]
13. Wang K, Shen T, Siegal GP, Wei S. The CD4/CD8 ratio of tumor-infiltrating lymphocytes at the tumor-host interface has prognostic value in triple-negative breast cancer. Hum Pathol 2017; 69: 110–7. [CrossRef]
14. Menter T, Bodmer-Haecki A, Dirnhofer S, Tzankov A. Evaluation of the diagnostic and prognostic value of PDL1 expression in Hodgkin and B-cell lymphomas. Hum Pathol 2016; 54: 17–24. [CrossRef]
15. Kinch A, Sundström C, Baecklund E, Backlin C, Molin D, Enblad G. Expression of PD-1, PD-L1, and PD-L2 in posttransplant lymphoproliferative disorder after solid organ transplantation. Leuk Lymphoma 2019; 60(2): 376–84. [CrossRef]
16. Berghoff AS, Ricken G, Widhalm G, Rajky O, Hainfellner JA, Birner P, et al. PD1 (CD279) and PD-L1 (CD274, B7H1) expression in primary central nervous system lymphomas (PCNSL). Clin Neuropathol 2014; 33(1): 42–9. [CrossRef]

17. Topalian SL, Hodi FS, Brahmer JR, Gettinger SN, Smith DC, McDermott DF, et al. Safety, activity, and immune correlates of anti-PD-1 antibody in cancer. N Engl J Med 2012; 366(26): 2443–54. [CrossRef]
18. Chen BJ, Chapuy B, Ouyang J, Sun HH, Roemer MG, Xu ML, et al. PD-L1 expression is characteristic of a subset of aggressive B-cell lymphomas and virus-associated malignancies. Clin Cancer Res 2013; 19(13): 3462–73. [CrossRef]
19. Muenst S, Hoeller S, Dirnhofer S, Tzankov A. Increased programmed death-1+ tumor-infiltrating lymphocytes in classical Hodgkin lymphoma substantiate reduced overall survival. Hum Pathol 2009; 40(12): 1715–22. [CrossRef]
20. Greaves P, Clear A, Owen A, Iqbal S, Lee A, Matthews J, et al. Defining characteristics of classical Hodgkin lymphoma microenvironment T-helper cells. Blood 2013; 122(16): 2856–63. [CrossRef]
21. Richendollar BG, Pohlman B, Elson P, Hsi ED. Follicular programmed death 1-positive lymphocytes in the tumor microenvironment are an independent prognostic factor in follicular lymphoma. Hum Pathol 2011; 42(4): 552–7. [CrossRef]
22. Wahlin BE, Aggarwal M, Montes-Moreno S, Gonzalez LF, Roncador G, Sanchez-Verde L, et al. A unifying microenvironment model in follicular lymphoma: outcome is predicted by programmed death-1--positive, regulatory, cytotoxic, and helper T cells and macrophages. Clin Cancer Res 2010; 16(2): 637–50. [CrossRef]
23. Ramsay AG, Clear AJ, Fatah R, Gribben JG. Multiple inhibitory ligands induce impaired T-cell immunologic synapse function in chronic lymphocytic leukemia that can be blocked with lenalidomide: establishing a reversible immune evasion mechanism in human cancer. Blood 2012; 120(7): 1412–21. [CrossRef]
24. Ahearne MJ, Bhuller K, Hew R, Ibrahim H, Naresh K, Wagner SD. Expression of PD-1 (CD279) and FoxP3 in diffuse large B-cell lymphoma. Virchows Arch 2014; 465(3): 351–8. [CrossRef]
25. Cohen M, Vistarop AG, Huaman F, Narbaitz M, Metrebian F, De Matteo E, et al. Cytotoxic response against Epstein Barr virus coexists with diffuse large B-cell lymphoma tolerogenic microenvironment: clinical features and survival impact. Sci Rep 2017; 7(1): 10813. [CrossRef]
26. Xu-Monette ZY, Zhou J, Young KH. PD-1 expression and clinical PD-1 blockade in B-cell lymphomas. Blood 2018; 131(1): 68–83. [CrossRef]
27. Furuse M, Kuwabara H, Ikeda N, Hattori Y, Ichikawa T, Kagawa N, et al. PD-L1 and PD-L2 expression in the tumor microenvironment including peritumoral tissue in primary central nervous system lymphoma. BMC Cancer 2020; 20(1): 277. [CrossRef]
28. Cho H, Kim SH, Kim SJ, Chang JH, Yang WI, Suh CO, et al. Programmed cell death 1 expression is associated with inferior survival in patients with primary central nervous system lymphoma. Oncotarget 2017; 8(50): 87317–28. [CrossRef]
29. Xu-Monette ZY, Xiao M, Au Q, Padmanabhan R, Xu B, Hoe N, et al. Immune profiling and quantitative analysis decipher the clinical role of immune-checkpoint expression in the tumor immune microenvironment of DLBCL. Cancer Immunol Res 2019; 7(4): 644–57.
30. Ciavarella S, Vegliante MC, Fabbri M, De Summa S, Melle F, Motta G, et al. Dissection of DLBCL microenvironment provides a gene expression-based predictor of survival applicable to formalin-fixed paraffin-embedded tissue. Ann Oncol 2018; 29(12): 2363–70. Erratum in: Ann Oncol 2019; 30(12): 2015. [CrossRef]